© 2014. Published by The Company of Biologists Ltd | Development (2014) 141, 1085-1094 doi:10.1242/dev.103333

RESEARCH ARTICLE

Developmental stratification of the mammary epithelium occurs through symmetry-breaking vertical divisions of apically positioned luminal cells

Robert J. Huebner[1], Terry Lechler[2] and Andrew J. Ewald[1,*]

ABSTRACT

Mammary ducts are elongated during development by stratified epithelial structures, known as terminal end buds (TEBs). TEBs exhibit reduced apicobasal polarity and extensive proliferation. A major unanswered question concerns the mechanism by which the simple ductal epithelium stratifies during TEB formation. We sought to elucidate this mechanism using real-time imaging of growth factor-induced stratification in 3D cultures of mouse primary epithelial organoids. We hypothesized that stratification could result from vertical divisions in either the apically positioned luminal epithelial cells or the basally positioned myoepithelial cells. Stratification initiated exclusively from vertical apical cell divisions, both in 3D culture and *in vivo*. During vertical apical divisions, only the mother cell retained tight junctions and segregated apical membranes. Vertical daughter cells initiated an unpolarized cell population located between the luminal and myoepithelial cells, similar to the unpolarized body cells in the TEB. As stratification and loss of apicobasal polarity are early hallmarks of cancer, we next determined the cellular mechanism of oncogenic stratification. Expression of activated ERBB2 induced neoplastic stratification through analogous vertical divisions of apically positioned luminal epithelial cells. However, ERBB2-induced stratification was accompanied by tissue overgrowth and acute loss of both tight junctions and apical polarity. Expression of phosphomimetic MEK (MEK1DD), a major ERBB2 effector, also induced stratification through vertical apical cell divisions. However, MEK1DD-expressing organoids exhibited normal levels of growth and retained apicobasal polarity. We conclude that both normal and neoplastic stratification are accomplished through receptor tyrosine kinase signaling dependent vertical cell divisions within the luminal epithelial cell layer.

KEY WORDS: Apicobasal polarity, Breast cancer, Epithelial development, Mammary gland, Mouse

INTRODUCTION

Simple epithelial cells are characterized by extensive intercellular junctions and strong polarity along the apicobasal axis (Bryant and Mostov, 2008; Zegers et al., 2003). This polarity is manifested both in specialized morphological features, such as apically localized microvilli, and by segregated plasma membrane domains with distinct apical and basolateral polarity proteins (Nelson, 2003; Yeaman et al., 1999). Yet these highly polarized cells emerge during development from less polarized, multilayered embryonic tissues. Early embryonic morphogenesis in the mammary and salivary glands is accomplished by a tissue with lower levels of polarity and adhesion than the mature epithelium in the adult organ (Andrew and Ewald, 2010; Hsu and Yamada, 2010). A fundamental and unresolved question in biology is how epithelial tissues transition between these different states of organization and polarity (Nelson, 2009). These transitions are also of biomedical interest, as epithelial tumors lose apicobasal polarity and simple organization early in cancer progression (Ewing, 1933), leading to the hypothesis that metastasis may involve reactivation of an embryonic developmental program (Hanahan and Weinberg, 2011; Thiery, 2002; Thiery et al., 2009; Yang and Weinberg, 2008).

The mammary gland is a powerful model system for studying transitions between simple and stratified epithelial organization, and for the corresponding changes in apicobasal polarity. The mammary ductal network arises during embryogenesis when the mammary placode invades the mammary mesenchyme (Hogg et al., 1983). During this invasion process the mammary epithelium is multilayered and few cells have contact with a luminal space or possess mature apicobasal polarity (Hogg et al., 1983; Nanba et al., 2001). At the end of fetal development the rudimentary ductal network repolarizes through unknown cellular mechanisms to form simple epithelial tubes with an inner luminal epithelial cell layer and a basally positioned myoepithelial cell layer (Hogg et al., 1983). These tubes then remain essentially quiescent until the arrival of circulating steroid hormones at the onset of puberty (Sternlicht et al., 2006).

Steroid hormone signals are mediated in the mammary gland through local receptor tyrosine kinase (RTK) interactions (Hennighausen and Robinson, 2005; McNally and Martin, 2011). One of the morphological consequences of RTK activation during puberty is the appearance of stratified terminal end buds (TEBs) at the tips of mammary ducts (Sternlicht, 2006). Cells within the TEB have low levels of cell adhesion and incomplete apicobasal polarity within the stratified cell layers (Ewald et al., 2008; Ewald et al., 2012; Mailleux et al., 2007). TEBs are the major site of proliferation during pubertal branching morphogenesis and accomplish ductal elongation (Hinck and Silberstein, 2005; Williams and Daniel, 1983). Genetic ablation of RTKs results in impaired TEB formation and delayed or abrogated ductal elongation (McNally and Martin, 2011; Sternlicht et al., 2006). We sought to determine how the stratified organization of the TEB arises from a simple bilayered epithelial duct and how stratification relates to loss of apicobasal polarity.

RESULTS

Growth factor signaling induces stratification of the mammary epithelium

We first sought to distinguish whether the stratified organization of the TEB emerges during puberty or persists from embryonic

[1]Departments of Cell Biology and Oncology, Center for Cell Dynamics, School of Medicine, Johns Hopkins University, 855 N. Wolfe Street, 452 Rangos Building, Baltimore, MD 21205, USA. [2]Duke University Medical Center, Departments of Cell Biology and Dermatology, Durham, NC 27710, USA.

*Author for correspondence (andrew.ewald@jhmi.edu)

Received 3 September 2013; Accepted 16 December 2013

Development (2014) doi:10.1242/dev.103333

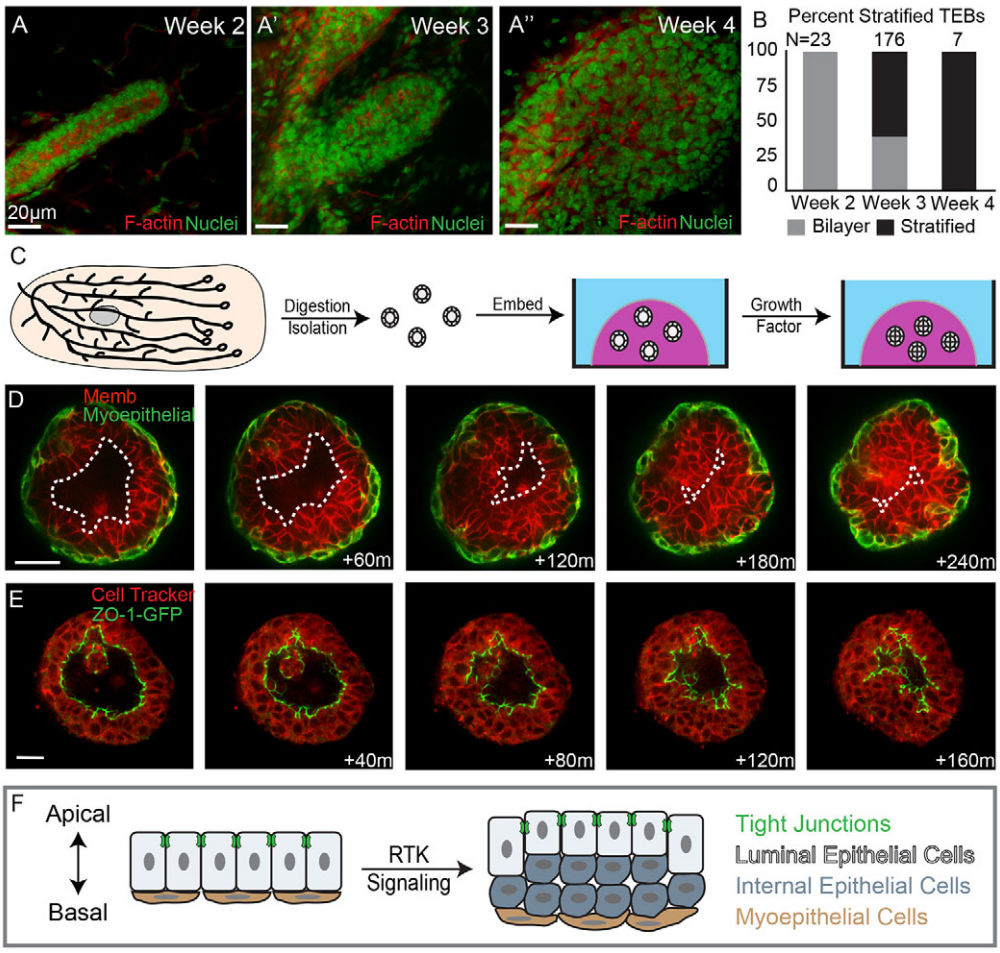

Fig. 1. Mammary stratification generates an internal population of luminal epithelial cells lacking tight junctions. (A-A″) Terminal end buds from 2- to 4-week-old mice were stained for F-actin (red) and nuclei (green). (B) Quantification of bilayered (gray) and stratified (black) end buds at 2, 3 and 4 weeks postnatal. (C) A schematic depicting organotypic culture. (D) Still images from a movie of an organoid undergoing stratification. Luminal epithelial cells are labeled red with a membrane localized tdTomato and myoepithelial cells are labeled green with a genetically encoded green fluorescent protein (GFP). The dashed line highlights the boundary of the luminal space. (E) Still images of an organoid undergoing stratification with ZO-1-GFP marking tight junctions and Cell Tracker Red staining the cytosol. (F) A cartoon depiction of mammary epithelial stratification showing the generation of an internal luminal epithelial cell population lacking tight junctions. Scale bars: 20 μm.

development. We collected a series of mammary glands from mice at 2 to 4 weeks of age and classified the ends of the primary mammary ducts as either bilayered or stratified, based on the number of luminal epithelial cell layers (Fig. 1A,B). We observed exclusively bilayered primary ducts before puberty (week 2, Fig. 1B). We observed a mixture of bilayered and stratified end buds at the onset of puberty (week 3, Fig. 1B). All end buds were stratified during early puberty (week 4, Fig. 1B). These data are consistent with earlier studies that noted polarized mammary tubes at birth (Hogg et al., 1983). Accordingly, we conclude that the stratified organization of the TEB emerges from a polarized, bilayered mammary duct, in response to RTK signaling at the onset of puberty. The result of this transition is an increase in the number of luminal epithelial marker+ cell layers. However, the cellular origin of these new luminal cells remains unclear.

We next sought to elucidate the cellular mechanism of TEB stratification. The slow timescale and optical inaccessibility of mammary development *in vivo* make it very difficult to image the cellular basis of developmental events within the intact mammary gland. This challenge led us to develop 3D organotypic culture and imaging techniques to enable real-time analysis of the cellular basis of mammary development (Ewald, 2013; Ewald et al., 2008; Ewald et al., 2012). Briefly, we isolate the epithelial ducts from primary mammary glands through a combination of mechanical disruption and enzymatic digestion and explant the resulting ‘mammary organoids’ into 3D gels of extracellular matrix (ECM) (Fig. 1C) (Nguyen-Ngoc et al., 2014). Branching morphogenesis is induced in mammary organoids in response to RTK signaling through addition of FGF or EGF ligands (Ewald et al., 2008; Fata et al., 2007).

Stratification resulted in generation of an internal luminal epithelial cell layer

We imaged FGF2-induced stratification in real time in organoids expressing a transgenically encoded myoepithelial-cell-specific fluorescent reporter (Vaezi et al., 2002) and a ubiquitous plasma membrane localized tdTomato (Muzumdar et al., 2007). We observed a monolayer of myoepithelial cells throughout stratification (Fig. 1D). By contrast, we observed a marked increase in the number of luminal epithelial cell layers, consistent with the 3D organization of the mammary TEB *in vivo* (Ewald et al., 2008; Mailleux et al., 2007). Mammary organoids therefore provide an observable model of developmental stratification.

During stratification, there was a large reduction in the volume of the lumen (Fig. 1D). Tight junctions are the apical most intercellular junction and mark polarized luminal epithelial cells. Tight junctions also regulate paracellular fluid permeability and partition apical and basolateral membranes (Schneeberger and Lynch, 2004). Stratification could occur through an incursion of cells past the tight junctions and into the luminal space or through the *de novo* generation of a third cell layer between the luminal and myoepithelial cells. To distinguish these possibilities, we imaged stratification in organoids expressing a tight junction reporter in which a fusion protein of green fluorescent protein (GFP) with zona occludens 1

Development (2014) doi:10.1242/dev.103333

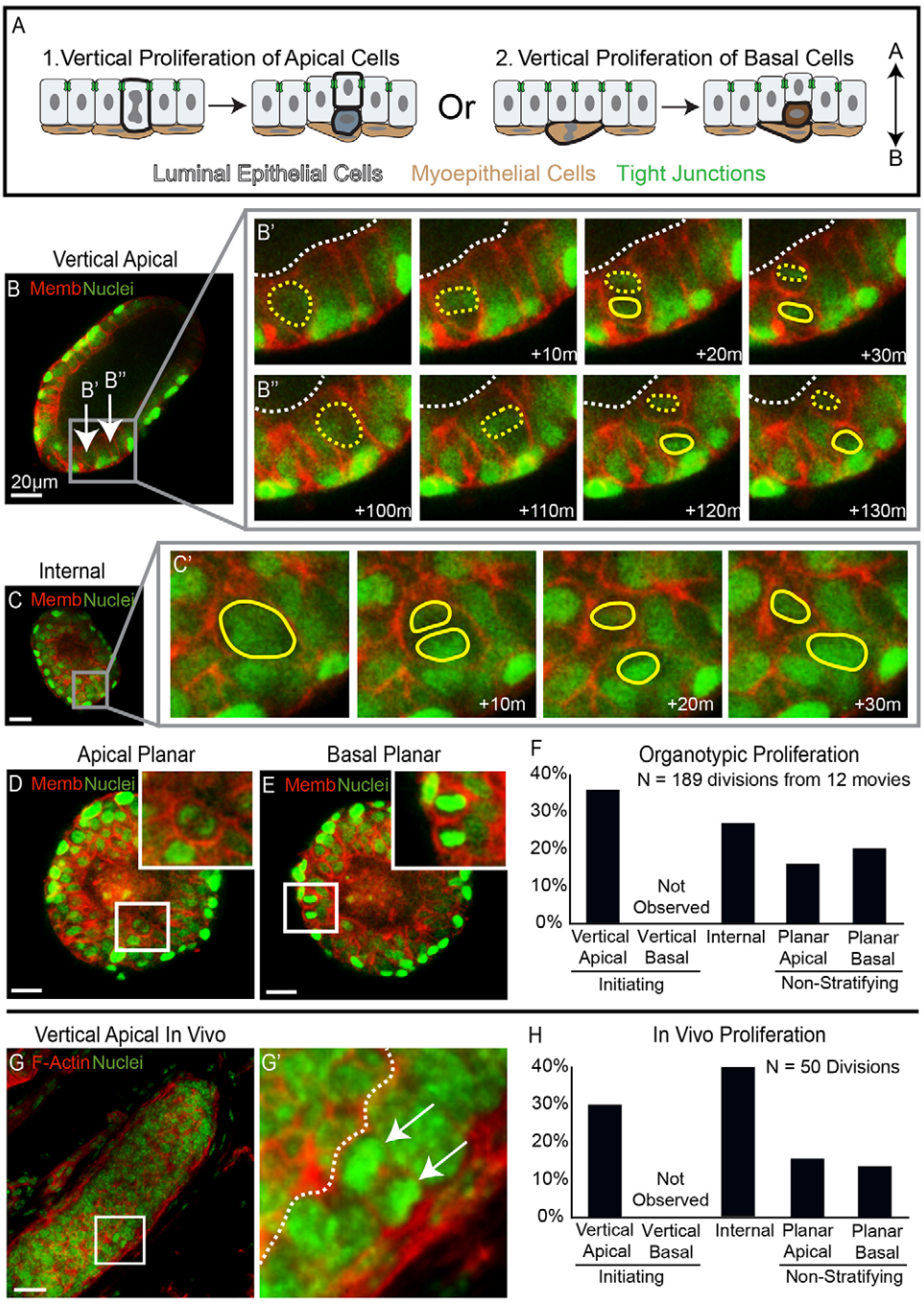

Fig. 2. Vertical apical cell divisions initiated mammary stratification. (A) A schematic depicting the alternatives of stratification initiation by vertical apical versus vertical basal proliferation. (B-E) Frames from movies of organoids expressing nuclear (green) and membrane (red) markers were collected to visualize proliferation in real time. (B) An image of an organoid before stratification. The arrows highlight apical cells that undergo vertical proliferation in B′ and B″. (B′,B″) Movie frames showing two vertical apical cell divisions, each producing one apical mother cell and one internal daughter cell. Yellow dashed lines show apical mother cells, solid yellow lines highlight internal daughter cells and dashed white lines represent the border of the lumen. (C) An organoid that is partially stratified with inset on an internal cell that divides in C′. (C′) Frames showing division of the internal cell highlighted in C; solid yellow lines outline the dividing nuclei. (D,E) An image of planar proliferation of apical and basal cells, respectively, insets on dividing cells. (F) Quantification of the types of proliferation observed in organotypic culture. (G) A terminal end bud from 3-week-old mouse stained for F-actin (red) and nuclei (green). The inset highlights a vertical apical division. (G′) An enlarged image of the inset from G; the arrows point to dividing nuclei and the dashed white line shows the border of the lumen. (H) Quantification of the types of proliferation observed *in vitro*. Scale bars: 20 μm.

(ZO-1-GFP) is knocked into the endogenous ZO-1 (TJP1 – Mouse Genome Informatics) allele. We observed reduction in luminal volume within the organoid, but ZO-1 was present at the lumen-facing surface of the most apical luminal epithelial cells throughout stratification in all movies (Fig. 1E). We occasionally observed dead cells within the lumen but did not observe migration of viable cells past the tight junctions. Our data reveal that a polarized, apically positioned luminal epithelial cell layer was maintained and that new cells arose between the apical and basal cell populations. At the end of stratification, organoids were composed of three structurally distinct cell populations, with a basal monolayer of myoepithelial cells, an apical layer of polarized luminal epithelial cells and a new internal cell population (Fig. 1F). Internal epithelial cells lacked contact with either the lumen or the basement membrane.

Developmental stratification initiates from vertical divisions of luminal epithelial cells

We hypothesized that internal epithelial cells could be generated through vertical proliferation of either apically positioned luminal epithelial cells or basally positioned myoepithelial cells (Fig. 2A). To distinguish these possibilities we imaged the location and direction of cell divisions in both populations using a dual transgenic fluorescent reporter mouse with nuclear and plasma membrane labels (Hadjantonakis and Papaioannou, 2004; Muzumdar et al., 2007). We classified the original cell based on its location and refer to it as the mother cell. We refer to the product of the cell division as the daughter cell. We analyzed 189 cell divisions to determine the origin of internal epithelial cells. We classified cell divisions based on the eventual location of the daughter cell through multiple time

Development (2014) doi:10.1242/dev.103333

points in three dimensions (3D). The additional information provided by the 3D volume was crucial to classifying cell division orientation. Vertical cell divisions were defined as those in which the daughter cell ended up in a different cell layer than the mother. Planar divisions were defined as those in which both the mother and the daughter cell occupied the same cell layer.

We observed frequent divisions in which an apically positioned luminal epithelial cell divided and only the mother cell remained in an apical position along the lumen lining surface (vertical apical, 68/189 total divisions, 68/99 apical divisions; Fig. 2B). These vertical apical cell divisions initiated stratification and produced internal daughter cells located between the polarized luminal and myoepithelial cell layers. Stratification was polyclonal as multiple vertical apical divisions were observed in the same organoid (8 of 12 movies; Fig. 2B-B″). We did not observe stratification initiating vertical divisions in the basally positioned myoepithelial cells (vertical basal, 0/189 total divisions, 0/39 basal divisions). Internal cells were also proliferative, further driving the stratification process (Fig. 2C). Both apically positioned luminal epithelial cells and basally positioned myoepithelial cells exhibited planar cell divisions with both mother and daughter cell remaining in the same cell layer (Fig. 2D,E). The percentage of each type of cell division was quantified, and vertical apical proliferation events were the most common during stratification (Fig. 2F). Altogether, more than 60% of proliferation during stratification resulted in the formation of an internal cell, either through vertical apical or internal cell proliferation.

To test if this mechanism of stratification was utilized *in vivo*, we fixed and sectioned mammary glands from 3-week-old mice and stained the tissue for nuclei and F-actin. We observed 15 examples of vertical apical proliferation events within TEBs *in vivo* (15/50 total divisions; Fig. 2G). Proliferation of internal cells was also observed *in vivo*, as well as planar proliferation of both apical and basal cells. No vertical basal proliferation events were observed *in vivo*. Quantification *in vivo* revealed that divisions resulting in an internal daughter cell accounted for ~70% of total proliferation (Fig. 2H). We conclude that the initiating step of developmental stratification is vertical division of luminal epithelial cells, both in 3D culture and *in vivo*.

Vertical apical divisions were accompanied by loss of polarity in the internal daughter

Vertical apical divisions produced a daughter cell located between the polarized luminal and myoepithelial cell layers. These internal epithelial cells displayed incomplete apicobasal polarity (Ewald et al., 2008; Ewald et al., 2012). We next sought to determine when this asymmetry in polarity emerged relative to cell division, through time-lapse imaging of organoids expressing ZO-1-GFP. During planar apical cell divisions, ZO-1-GFP remained punctate and apically localized in both the mother and daughter cell (Fig. 3A). By contrast, during vertical apical cell divisions the ZO-1-GFP signal was only observed at the apical membrane of the mother cell (80/80 divisions; Fig. 3B). Accordingly, we conclude that the internal daughter cell is generated without ZO-1 containing tight junctions.

Tight junctions play a crucial role in partitioning the apical from the basolateral membrane and enabling stable segregation of apical and basolateral polarity complexes (Schneeberger and Lynch, 2004). At the apical surface the Par complex [PAR-3 (PARD3 – Mouse Genome Informatics), aPKC and CDC42] regulates apical identity and is required for mammary morphogenesis (McCaffrey and Macara, 2009). Conversely the Scribble complex (scribble, lethal giant larvae and discs large) regulates basolateral identity and its loss promotes mammary tumorigenesis (Zhan et al., 2008). We next used antibodies to determine the localization of apical and basal polarity complexes during vertical apical cell divisions. PAR-3 was localized at the apical membrane of the mother cell and within the cytosol of the internal daughter cell (Fig. 3C). Scribble was excluded from the apical membrane between the tight junctions and localized to the basolateral membranes of the mother cell and all cell membranes of the internal daughter cell (Fig. 3D). In *Drosophila*, the Numb protein localizes asymmetrically within the sensory organ precursor and directs differential cell fates for the two daughter cells (Rhyu et al., 1994). During vertical apical divisions in the mammary epithelium, numb localized in a crescent along the basal surface of the internal daughter cell (Fig. 3E). We conclude that the mother cell retains tight junctions and molecularly distinct apical and basolateral membranes during vertical apical cell divisions. By contrast, internal daughter cells lacked tight junctions, displayed cytosolic PAR-3, and localized scribble throughout the plasma membrane. We conclude that the internal daughter cells of vertical apical divisions are generated without the apicobasal polarity or junctional complexes typical of polarized simple epithelial cells.

Oncogenic stratification initiates from vertical apical cell divisions

Stratification and loss of polarity in a simple epithelium are also early events in the progression of epithelial cancers (Ewing, 1933; Huang and Muthuswamy, 2010). We next sought to determine if oncogenic stratification utilized the same cellular mechanism as developmental stratification. To answer this question, we induced hyperplasia formation through expression of an activated form of ERBB2 (Xie et al., 1999). Activated ERBB2 was expressed under the control of a two-allele tetracycline regulation system (Fig. 4A). The first allele encoded the reverse tetracycline transactivator (rtTA), an internal ribosomal entry site (IRES), and EGFP, both downstream of a *loxP*-flanked stop codon. The second allele coded the activated form of ERBB2 downstream of a tetracycline operator. Adenoviral delivery of Cre recombinase enabled mosaic expression of rtTA and EGFP and addition of doxycycline then led to ERBB2 expression (Fig. 4B). Tet-regulated expression of activated ERBB2 drives epithelial stratification *in vivo* (Xie et al., 1999) and ERBB2 expression is sufficient to cause proliferation of human mammary epithelial cells (Muthuswamy et al., 2001).

Expression of activated ERBB2 was also sufficient to induce proliferation and epithelial stratification in mammary organoids. We next collected time-lapse movies of control and activated ERBB2-expressing organoids to elucidate the cellular mechanism of oncogenic stratification. Organoids grown without exogenous growth factor remained bilayered (Fig. 4C,C′). Expression of activated ERBB2 resulted in stratification and disorganized growth of organoids, even without exogenous growth factor (Fig. 4D,D′). We measured growth rates to quantify the extent of organoid growth following ERBB2 expression. Organoids expressing activated ERBB2 grew at a much faster rate than control organoids treated with growth factor (Fig. 4E). ERBB2-driven tissue growth was accomplished by an expansion in the number of luminal cell layers, whereas the myoepithelium remained in a complete monolayer (Fig. 4F, smooth muscle actin staining, green).

To isolate the cellular mechanism responsible for oncogenic stratification, we next visualized the location and direction of cell divisions. Vertical apical cell divisions were frequently observed to initiate stratification in response to activated ERBB2 expression (Fig. 4G,H). We did not observe vertical basal cell divisions. Planar proliferation was observed in both apically positioned luminal epithelial cells and basally positioned myoepithelial cells (Fig. 4G).

Development (2014) doi:10.1242/dev.103333

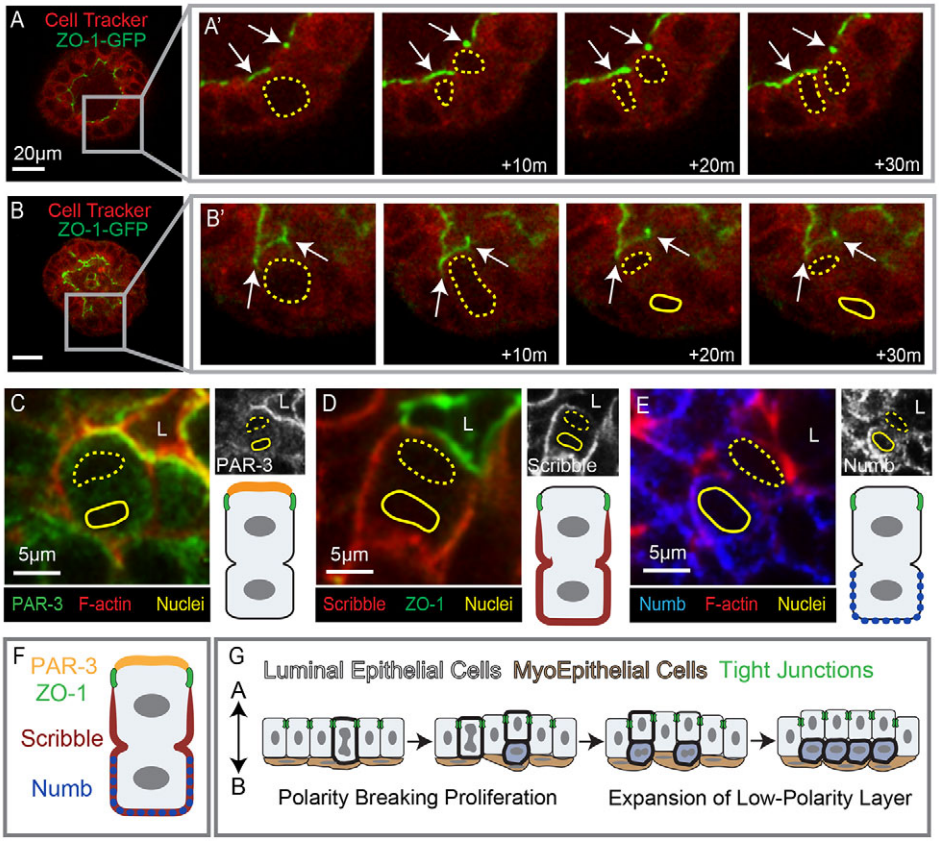

Fig. 3. Vertical apical cell divisions result in polarity loss for internal daughter cells. (A-B′) Frames from movies of a ZO-1-GFP-expressing organoid (green) counterstained with Cell Tracker Red. (A) An organoid undergoing stratification; the inset highlights a cell that undergoes planar apical proliferation in A′. (A′) Magnification of the inset from A; arrows point to tight junctions, which were apically localized during apical proliferation. Yellow dashed lines highlight both the mother and the daughter cell. (B) A still image of an organoid with inset on an apical cell before the vertical division shown in B′. (B′) Images show the asymmetric localization of ZO-1 to the apically positioned mother cell during vertical apical cell division. Yellow dashed lines emphasize the mother cell; solid lines show the internal daughter cell and arrows point to the tight junctions. (C-E) Immunofluorescence staining of apical cells during vertical divisions. The luminal space is marked L, apical nuclei are highlighted with dashed yellow lines and internal nuclei are shown with solid yellow lines. Black and white images of the respective polarity proteins are shown in the upper right and a schematic depiction of the protein localization is included in the bottom right. (C) PAR-3 was asymmetrically localized to the apical membrane of the mother cell during vertical division. (D) The basolateral polarity protein scribble was excluded from the ZO-1 defined apical domain but was present on all other basolateral surfaces. (E) Numb was enriched in the basolateral membranes of the daughter cell. (F) A cartoon depiction of the asymmetric localization of polarity proteins during vertical apical cell divisions. (G) A schematic depicting the cellular mechanism of mammary stratification initiating with polarity breaking vertical apical cell divisions followed by expansion of the low-polarity internal cell layer. Scale bars: 20 μm unless otherwise noted.

Internal epithelial cells were also highly proliferative. In total, ~60% of cell divisions observed in organoids expressing activated ERBB2 resulted in generation of an internal daughter cell (sum of vertical apical and internal divisions; Fig. 4G). We conclude that expansion of the luminal epithelial compartment following expression of activated ERBB2 is typically accomplished via vertical divisions of apically positioned luminal epithelial cells.

Developmental stratification resulted in generation of low-polarity internal epithelial cells, located between a polarized luminal epithelial cell layer and the myoepithelial cells (Fig. 4I,K). We next assayed for molecular polarity in stratified hyperplasias induced by expression of activated ERBB2. PAR-3 and ZO-1 staining indicated that apical polarity was acutely disrupted by activated ERBB2, consistent with reports in epithelial cell lines (Muthuswamy et al., 2001). Punctate ZO-1 was absent from the plasma membranes adjacent to luminal spaces and the ZO-1 that was detected was largely cytosolic (Fig. 4L). Similarly, PAR-3 was absent from the lumen-facing surface of the plasma membrane (Fig. 4J). The majority of PAR-3 was cytosolic in organoids expressing activated ERBB2. These results reveal that ERBB2-induced and developmental stratification both occur through vertical division of apical cells and that ERBB2 activation additionally leads to unrestrained growth and loss of apicobasal polarity.

MEK1DD-induced stratification initiates from vertical apical cell divisions

Developmental stratification is induced through ligand-dependent RTK signaling, whereas activated ERBB2 drives RTK signaling in a ligand-independent fashion. The tissue overgrowth and loss of polarity associated with activated ERBB2 could therefore result from continuous activation of downstream RTK pathway components. To determine whether intrinsic stimulation of proliferation was sufficient to result in tissue overgrowth, we induced expression of an activated form of a mitogen-activated protein kinase (MAPK), a downstream effector of RTK signaling. We used a genetic approach to express a constitutively active mutant of MEK1 (MAP2K1 – Mouse Genome Informatics) called

Development (2014) doi:10.1242/dev.103333

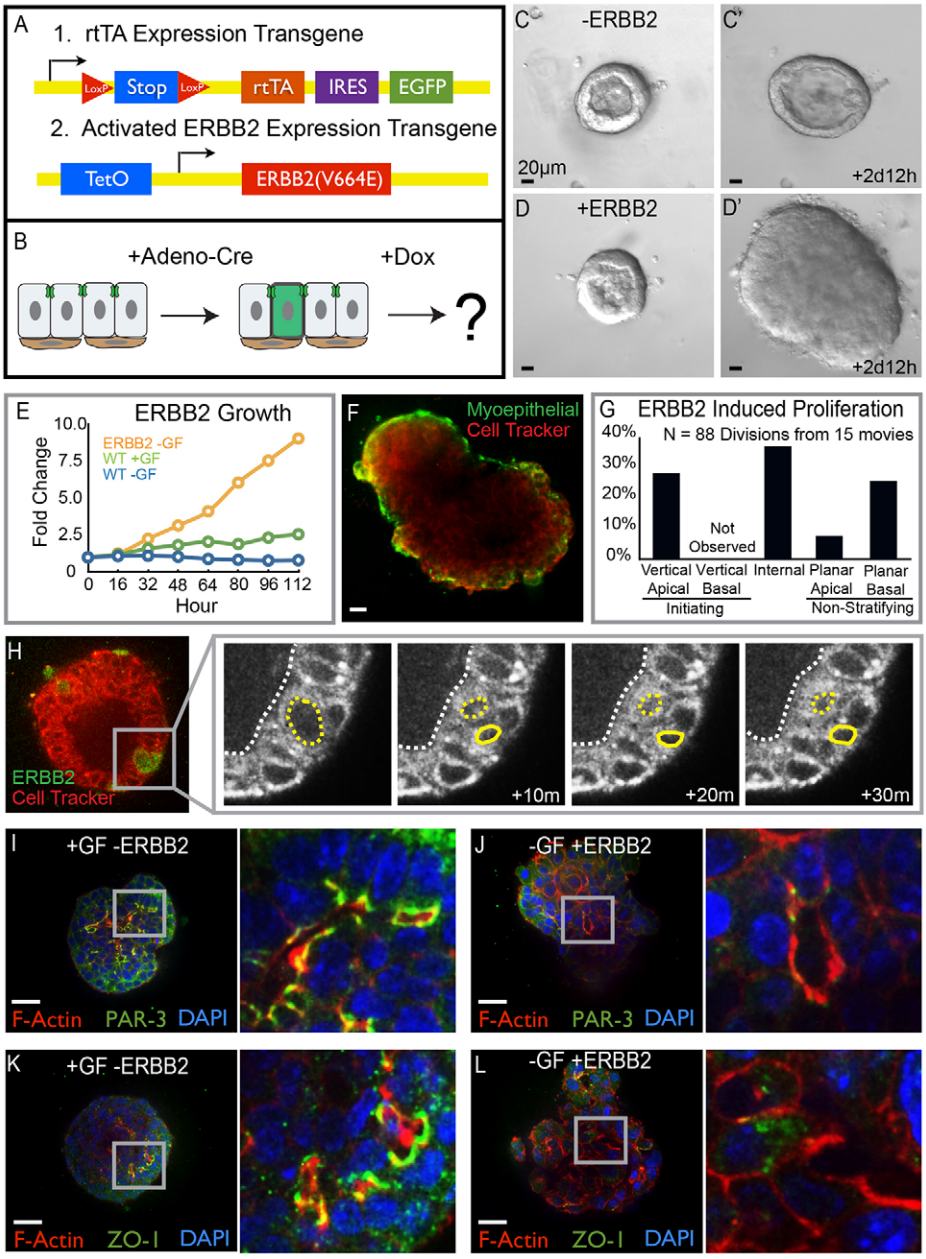

Fig. 4. Oncogenic stratification shares a conserved cellular mechanism with developmental stratification. (A) Schematic of the transgenes used for conditional and mosaic expression of activated ERBB2. (B) Cartoon depicting the protocol followed to drive ERBB2 expression. (C-D′) Still images from time-lapse movies of unstimulated organoids in the presence or absence of ERBB2 expression. (C,C′) Organoids remained bilayered in the absence of ERBB2. (D,D′) Expression of ERBB2 in 80-90% of cells resulted in rapid stratification and growth. (E) Organoid growth rates were quantified as the increase in organoid area normalized to the initial organoid size. Growth curves for organoids expressing activated ERBB2 without exogenous growth factor are shown in orange, for control organoids with growth factor are shown in green, and for control organoids without exogenous growth factor are shown in blue. (F) Organoids expressing ERBB2 in 80-90% of cells were fixed and stained for smooth muscle actin (SMA, green), 3 days after gene activation. SMA, a marker of myoepithelial cells, showed that ERBB2-induced stratification increased the number of luminal epithelial cell layers. (G) Quantification of the types of cell divisions observed in ERBB2-expressing organoids. (H) Mosaic expression of ERBB2 in 1-10% of cells allowed observation of individual cellular responses to oncogene activation. ERBB2-expressing cells were labeled with GFP (green) and Cell Tracker Red was used to infer nuclear location. ERBB2-induced stratification initiated from vertical apical cell divisions. (I-L) Tissue was fixed and stained 3 days after addition of growth factor or activation of ERBB2 in 80-90% of cells. (I,J) Apical polarity was visualized by staining for PAR-3 (green) as well as F-actin (red) and nuclei (blue). (I) Polarized apical membranes were present at the apical surfaces of tissue treated with growth factor. (J) Tissue expressing ERBB2 lacked membrane localized PAR-3. (K,L) ZO-1 staining (green) was used to observe tight junctions; tissue was also stained for F-actin (red) and nuclei (blue). (K) Growth factor-treated organoids had ZO-1 localized to apical membranes. (L) Tight junctions were absent from apical membranes in cells expressing ERBB2; the inset shows a region of tissue lacking tight junctions. Scale bars: 20 μm.

MEK1DD (Srinivasan et al., 2009). The transgenic mouse line was engineered to enable expression of MEK1DD and EGFP following Cre-recombinase-mediated excision of a *loxP*-flanked stop site (Srinivasan et al., 2009). We used adenovirally delivered Cre to enable expression of MEK1DD in fluorescently labeled mosaic clones within primary mammary epithelial organoids.

Expression of MEK1DD was sufficient to induce proliferation and stratification in the absence of exogenous growth factor (Fig. 5A,B). Stratification resulted in multiple luminal epithelial layers and a monolayer of myoepithelial cells (Fig. 5C). MEK1DD expression induced a similar growth rate as that observed following addition of growth factor to control organoids (Fig. 5B). We next used time-lapse confocal microscopy to identify the cellular mechanism of stratification. MEK1DD-induced stratification also initiated from vertical apical cell divisions and we did not observe vertical basal divisions (Fig. 5D,E). In contrast to the loss of polarity observed following activated ERBB2 expression, MEK1DD-expressing organoids maintained apical-basal polarity comparable to growth factor-stimulated control organoids (Fig. 5F,G).

MEK and PI3 kinase are both required for activated ERBB2-induced proliferation

We demonstrated that both growth factor-induced and ligand-independent activation of RTK signaling induced stratification through vertical apical cell divisions. However, activated ERBB2 induced both higher levels of proliferation and loss of apicobasal polarity, compared with expression of MEK1DD. ERBB2 signals through both the MAPK and PI3K/AKT pathways. We therefore tested which of these two pathways were responsible for the excess proliferation observed following expression of activated ERBB2. Organoids were allocated to a control and three experimental groups, all of which received doxycycline. Control organoids were infected with Adeno-GFP and therefore could not express the rtTA. Experimental organoids were infected with Adeno-Cre, leading to

Development (2014) doi:10.1242/dev.103333

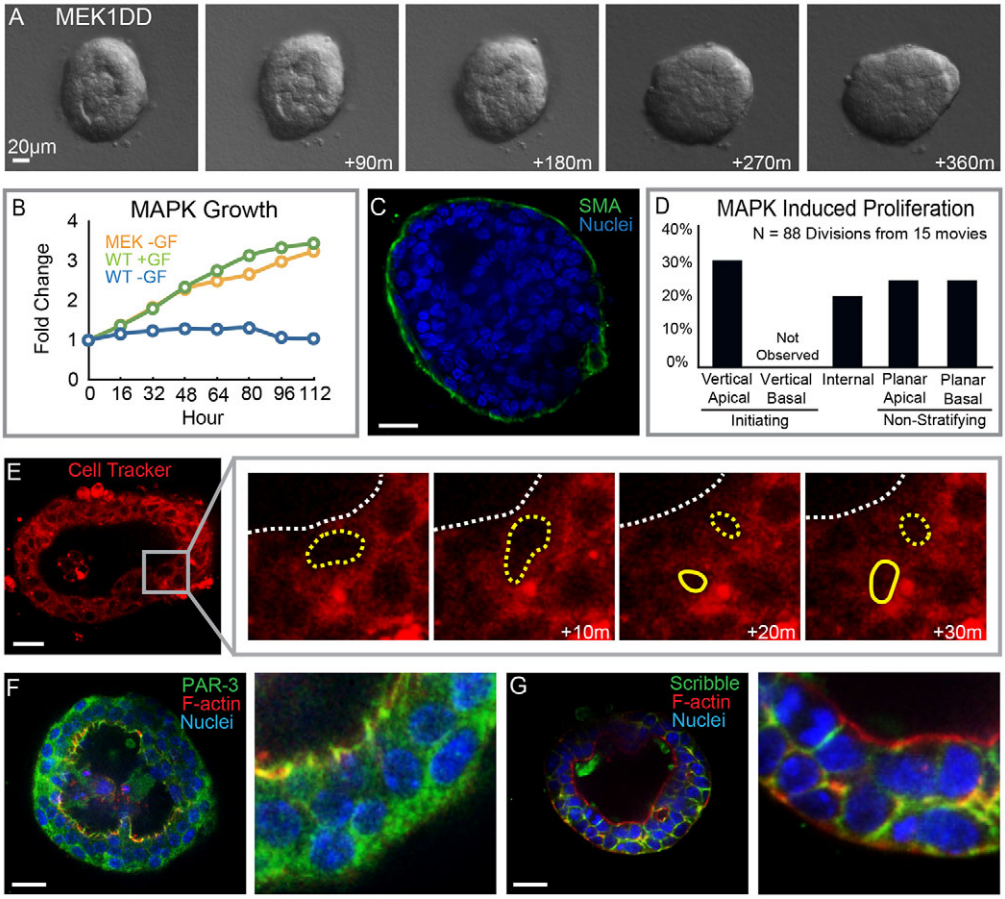

Fig. 5. MEK1DD-induced stratification through vertical apical cell divisions. (A) Still images from a time-lapse movie of organoids expressing a phosphomimetic form of MEK (MEK1DD). MEK1DD expression was sufficient to drive stratification. (B) Growth curves for organoids expressing MEK1DD without exogenous growth factor are shown in orange, for control organoids with growth factor in green and for organoids without exogenous growth factor in blue. (C) MEK1DD-expressing organoids were stained for SMA (green) and nuclei (blue) to visualize the myoepithelial cells. (D) Quantification of the types of proliferation observed in response to MEK1DD expression. (B) MEK1DD-induced stratification was initiated by vertical apical cell divisions; organoids were stained with Cell Tracker Red to infer nuclear position. (F) Organoids were stained for PAR-3 (green) F-actin (red) and nuclei (blue) to visualize apical polarity. (G) Organoids were stained for scribble (green) F-actin (red) and nuclei (blue) to visualize basolateral polarity. Scale bars: 20 μm.

expression of an rtTA and activated ERBB2. A subset of experimental organoids were treated with either MEK inhibitor (U0126) or PI3K inhibitor (LY294002). After 3 days, organoids were fixed and stained for the mitosis marker phospho-histone H3 (PH3) and 4′,6-diamidino-2-phenylindole (DAPI) to mark all nuclei. The percentage of proliferating cells per organoid was calculated as the ratio of PH3-positive cells to total cells. Control organoids exhibited low levels of proliferation (Fig. 6B,C), and expression of activated ERBB2 induced a significant increase in proliferation (Fig. 6B,D). Addition of either MEK inhibitor or PI3K inhibitor decreased proliferation below the control baseline (Fig. 6B,E,F). We conclude that MEK and PI3K are independently required for ERBB2-induced proliferation.

DISCUSSION

The mammary epithelium represents a unique model system in which to study transitions in epithelial architecture, as the postnatal mammary duct is polarized and simple, while the elongation of these ducts is accomplished by stratified TEBs (Hinck and Silberstein, 2005; Williams and Daniel, 1983). These transitions occur in response to steroid hormone and RTK signaling (Sternlicht et al., 2006). Whereas genetic requirements for ductal elongation have become increasingly clear (McNally and Martin, 2011), the cellular basis of the simple to stratified transition has remained obscure.

Our data reveal that developmental stratification initiates from vertical division of apically positioned luminal epithelial cells in 3D culture and *in vivo* in TEBs. We observed no stratification-inducing divisions within the basally positioned myoepithelial compartment. Internal daughter cells lacked tight junctions and molecularly segregated apical membrane domains. Generation of the internal cell layer was not clonal, as multiple vertical apical divisions occurred in individual organoids. Stratification was also initiated by vertical apical divisions in organoids expressing activated forms of ERBB2 or MEK1. However, expression of activated ERBB2 additionally induced tissue overgrowth and acute loss of apical polarity and required both MEK and PI3K activity. The differences in phenotypes between ERBB2 and MEK expression could result from this utilization of multiple proliferation pathways or from differences in levels of MEK activation. Alternately, ERBB2 itself could be involved in polarity loss through direct interactions between ERBB2 and PAR6-aPKC (Aranda et al., 2006).

Epithelial isolation and transplantation studies based on cell surface markers defined the mammary epithelial populations capable of single cell, long-term repopulation. These studies suggested that long-term repopulating cells may express basal epithelial markers (Vaillant et al., 2007; Visvader and Smith, 2011). Accordingly, it was reasonable to expect a contribution of basal cells to stratification. One recent study revealed exclusively planar cell divisions within the basal, cap cell layer of the TEB, with no observed contribution of basal cells to the internal, body cell compartment (Taddei et al., 2008). Another recent study observed a minority of vertical basal cell divisions in stratified TEBs during ductal elongation (Regan et al., 2013). Both of these studies were based on the analysis of fixed sections of the mammary gland. Cell division orientation can be difficult to analyze in 2D in fixed sections, as spindle orientation can rotate extensively during mitosis *in vivo* (Kieserman and Wallingford, 2009). By contrast, we were able to follow the entire process of mitosis in 3D in real time. Our

Development (2014) doi:10.1242/dev.103333

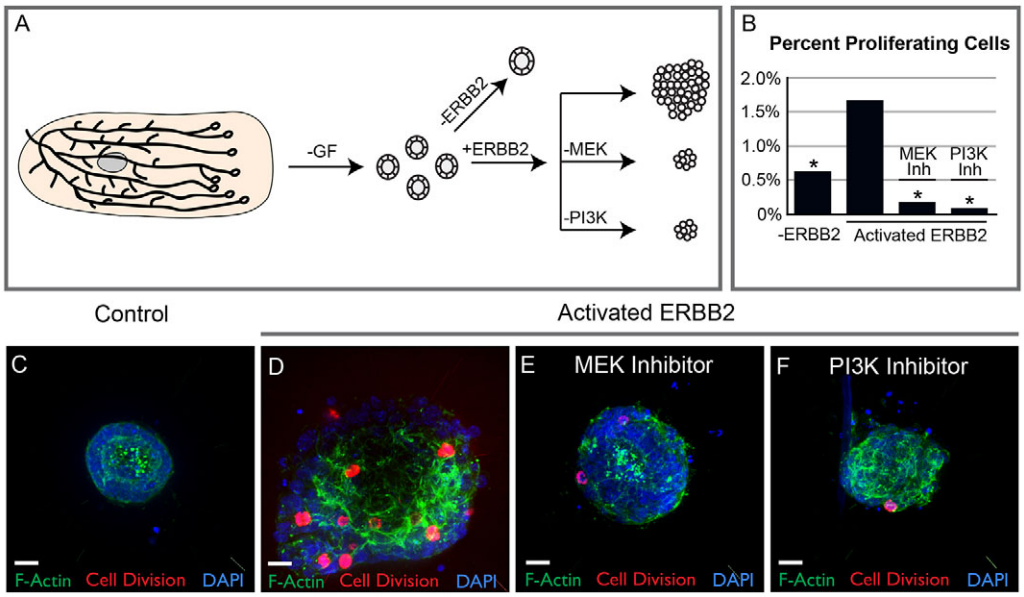

Fig. 6. MAPK and PI3 kinase are both required for ERBB2-induced proliferation. (A) Organoids were allocated to control and ERBB2-expressing experimental groups. A subset of the ERBB2-expressing organoids were treated with either MEK or PI3 kinase inhibitor. (B) Organoids were fixed 3 days after ERBB2 activation and stained for the proliferation marker PH3 (red), DAPI (blue) and F-actin (green). Quantification of the effect of MEK and PI3 kinase inhibitors on organoids expressing mutant ERBB2. Percent proliferation was quantified as the number of PH3-positive cells divided by the total number of cells per organoid. Stars highlight conditions that were significantly different by ANOVA (P<0.001) from the activated ERBB2 mutant. (B) Control organoids displayed a low level of proliferation. (C) ERBB2 activation increased the number of PH3-positive cells. (C) MEK inhibition with U0126 (U) decreased proliferation below the level observed in control organoids. (D) Inhibition of the AKT pathway with the PI3 kinase inhibitor LY294002 (LY) decreased proliferation below the level of control organoids. Scale bars: 20 μm.

data do not exclude the possibility of infrequent contributions to the stratified body cell compartment from basally positioned stem cells. However, our data suggest that vertical apical divisions are the typical mechanism for initiation of epithelial stratification. We cannot distinguish whether vertical apical divisions are actively induced or whether a signal that would normally constrain cell divisions to the planar direction is repressed.

This mechanism of stratification from the apical side is in contrast to that observed in other epithelial organs in which stratification initiates exclusively from basally positioned cells (Lechler and Fuchs, 2005). Within the embryonic skin, stratification initiates when cells rotate their division axis from parallel with the ECM to perpendicular, thereby generating suprabasal cells (Lechler and Fuchs, 2005). Suprabasal cells proliferate and differentiate apically until terminal differentiation, cell death and eventual sloughing off of the body (Fuchs, 2007). The organization of the lung epithelium is also regulated by the angle of the mitotic spindle and oncogenic signals disrupt normal lung structure in part by changing spindle angle (Tang et al., 2011). Oncogenic stimuli can also induce multilayered epithelial structures through migration of cells into the luminal space (Leung and Brugge, 2012; Yagi et al., 2012). Accordingly, we anticipate that our observed mechanism of vertical apical cell divisions might be most common in cancers in which the driving molecular event is deregulated RTK signaling. 3D culture models of mammary cancer have also provided insight into the cellular response to ERBB2 activation. Ubiquitous expression of ERBB2 was sufficient to induce stratification in mature acini of non-transformed mammary epithelial cells (MCF10A) (Muthuswamy et al., 2001). Mosaic expression of ERBB2 in mature MCF-10A acini resulted in cell migration into the lumen (Leung and Brugge, 2012). However, MCF-10A cells do not form tight junctions or establish bilayered tubes with defined luminal and myoepithelial cells (Underwood et al., 2006). The additional developmental constraints of tight junctions and myoepithelial-luminal epithelial cell interactions may prevent migration into the lumen, regulate the orientation of cell division, and determine the eventual location of the daughter cell.

We conclude that epithelial stratification can rapidly occur through vertical divisions of polarized, apically positioned luminal epithelial cells and that stratification is typically coincident with loss of tight junctions and apicobasal polarity in the internal daughters. Our data therefore reveal a readily accessible developmental program that can be activated to yield two characteristic features of epithelial cancers: stratification and loss of polarity.

MATERIALS AND METHODS

Transgenic fluorescent reporter animals

Myoepithelial cells were visualized in real time by transgenic expression of GFP under the control of the keratin-14 promoter (Vaezi et al., 2002); these mice were a kind gift from Elaine Fuchs. Membranes were labeled by membrane-targeted mTomato, expressed from the *rosa26* locus; mice were acquired from the Jackson Laboratory (Muzumdar et al., 2007). Transgenic mice expressing Histone H2B-GFP were acquired from AK Hadjantonakis, Memorial Sloan Kettering, and were used to follow proliferation in real time (Hadjantonakis and Papaioannou, 2004). All mouse procedures were conducted in accordance with an approved protocol from the Institutional Animal Care and Use Committee, Johns Hopkins University.

ZO-1-GFP knock-in animals

Targeting constructs and embryonic stem cell electroporation were performed by the Duke Recombineering Core and Transgenic animal facilities. GFP was inserted in frame immediately before the stop codon of

ZO-1. The resulting strain Tjm1tm1(IF-GFP)Lech was viable with no observed phenotype even when maintained as a homozygote.

Organotypic culture

Three-dimensional culture of primary mammary epithelium was performed as previously described (Ewald et al., 2008; Nguyen-Ngoc et al., 2014). Briefly, mammary glands were removed from 8- to 12-week-old mice and tissue was minced 40-50 times with a scalpel. The epithelial compartment was separated from the stromal tissues through collagenase and DNase digestion. Differential centrifugation was used to separate epithelial organoids from single cells. The final pellet was suspended in growth factor reduced Matrigel (BD Biosciences) at a concentration of two organoids/µl and plated as 100 µl drops in 24-well glass bottom plates (Greiner Bio One). Matrigel drops were allowed to solidify for 20 minutes at 37°C before addition of minimal media. Growth factor was added at the time of plating (FGF2, 2.5 nM), unless otherwise noted. Cell Tracker Red was added, when required, as previously described (Ewald et al., 2008).

Adenoviral gene delivery

Organoids were treated with adenoviral-Cre or adenoviral-GFP (Vector Biolabs) before suspension in Matrigel. Following differential centrifugation, 1000 organoids were transferred to a 1.7 ml Eppendorf tube and centrifuged at 520 ***g*** for 10 minutes. All but 100 µl of media was then removed from the Eppendorf tube. Viral particles were added to the organoid-containing media and incubated for 1 hour. Two viral concentrations were used: 10,000 plaque-forming units (PFU) or 500 PFU per organoid. The high concentration of virus resulted in ~80% infection and the low concentration produced two to ten infected cells per organoid. Following viral treatment, organoids were washed twice in DMEM-F12 and suspended in Matrigel as previously described.

Whole gland and organoid antibody staining

Whole mammary glands were removed from 2- to 4-week-old mice and fixed in 4% paraformaldehyde (PFA) for 20 minutes. Tissue was embedded in optimal cutting temperature (OCT) compound (Tissue-Tek) and cut as 50 µm sections. Sectioned tissue was washed with phosphate-buffered saline (PBS) to remove excess OCT and permeabilized with 0.5% Triton X-100 for 30 minutes. Epithelium was stained with DAPI (Invitrogen, 1:1000) to visualize nuclei and phalloidin (Invitrogen, 1:500) to visualize F-actin. Slides were washed in PBS and mounted. Organoid staining for PAR-3 (Millipore, 07-330), numb (Cell Signaling Technology, C29611), scribble (Santa Cruz Biotechnology, sc-11049), ZO-1 (Chemicon, MAB1520), and SMA (Sigma, F3777) was performed as described in (Ewald et al., 2012). Briefly, organoids were fixed with 4% PFA for 20 minutes and permeabilized in 0.5% Triton X-100 for 30 minutes. Organoids were blocked in 10% serum in PBS for 3 hours and then incubated with primary antibody (1:500 in 10% serum in PBS) for 2 hours. Organoids were washed three times with 10% serum in PBS and then incubated with Alexa Fluor conjugated secondary antibodies (Molecular Probes, 1:500) in 10% serum in PBS for 1 hour. DAPI (1:1000) and phalloidin (1:500) staining were performed concurrently with secondary antibodies. Three 10-minute PBS washes were applied and organoids were analyzed by confocal microscopy.

ERBB2 and MEK activation assays

A dual transgenic mouse line was used to conditionally and mosaically express constitutively activated ERBB2 in mammary epithelium. The first transgenic mouse coded both an rtTA and EGFP downstream a *loxP*-flanked stop codon (Belteki et al., 2005). The second allele coded an activated form of rat ERBB2 regulated by the tetracycline operator (Xie et al., 1999). Both lines were acquired from Jackson Laboratories. Adeno-Cre was added as described above, resulting in mosaic expression of rtTA and EGFP. Doxycycline was added at 5 µg/ml at 24 hours after plating to induce ERBB2 expression. ERBB2-expressing organoids were grown in the absence of exogenous growth factors. All ERBB2 experiments were internally controlled with organoids from the same animal. Control organoids received Adeno-GFP in place of Adeno-Cre and were treated with doxycycline. In cases where ERBB2-expressing organoids were compared to growth factor stimulated organoids, growth factor was added 24 hours after plating.

An activated mutant of MEK1, with serine to aspartic acid substitutions at residues S218 and S222 (MEK1DD), was expressed to drive constitutive MAPK signaling. MEK1DD was expressed under the control of the *rosa26* promoter, upstream of an IRES-EGFP and downstream of a *loxP*-flanked stop codon. Mice were acquired from Jackson Laboratories (Srinivasan et al., 2009). Addition of Adeno-Cre, as described above, resulted in expression of the MEK mutant and EGFP. Tissue expressing MEK1DD did not receive exogenous growth factors. MEK experiments were internally controlled with organoids from the same animal treated with Adeno-GFP instead of Adeno-Cre. Growth factor was added at the time of plating to compare with the MEK-expressing organoids.

MEK and PI3 kinase inhibition assays

The MEK inhibitor U0126 was acquired from Cell Signaling and used at 10 µM. PI3 kinase was inhibited with 50 µM of LY294002, which was obtained from Cell Signaling. Organoids were pretreated with MEK or PI3K inhibitors for 30 minutes before *Erbb2* gene induction. Organoids were fixed 3 days after inhibitor addition and stained for the nuclear marker DAPI and the proliferation marker PH3 (Cell Signaling, 9701). Percent proliferating cells per organoid was quantified as the number of PH3-positive cells divided by the total number of cells in the organoid. A single factor analysis of variance was used to determine statistical significance ($P<0.001$) and a minimum of 20 organoids per condition from three independent experiments was analyzed.

Confocal microscopy

Still and time-lapse confocal images were collected using a Solamere Technology Group spinning disk confocal microscope (Ewald, 2013) with a 40× LD-LCI C-Apochromat objective (Zeiss Microimaging). A combination of µManager (Edelstein et al., 2010) and Piper (Stanford Photonics) imaging software was used for imaging acquisition. Images were recorded with a 10-minute interval for 8-16 hours. Temperature was held at 37°C and CO_2 was 5% throughout imaging. Imaris (Bitplane) and Adobe Photoshop were used to adjust brightness and contrast across the entire image field, to optimize image clarity.

Time-lapse differential interference contrast microscopy

A Zeiss Cell Observer system with a Zeiss AxioObserver Z1 and an AxioCam MRM camera was used to collect differential interference contrast microscopy movies. Movies were collected with a 20-minute time interval. Imaging began upon addition of growth factor or gene induction and continued until ~5 days after growth stimulation. Temperature was maintained at 37°C and CO_2 was held at 5%.

Acknowledgements

We thank Neil Neumann and Eliah Shamir for critical comments on the manuscript and Jen Beck for technical assistance.

Competing interests

The authors declare no competing financial interests.

Author contributions

A.J.E. and R.J.H. designed the experiments. R.J.H. conducted the experiments. A.J.E. and R.J.H. analyzed the data, built the figures and wrote the manuscript. T.L. developed the ZO-1-GFP mouse strain and edited the manuscript.

Funding

A.J.E. was supported by a Research Scholar Grant [RSG-12-141-01 – CSM] from the American Cancer Society; R.J.H. was supported by a National Institutes of Health (NIH)/NIGMS training grant [2T32GM007445]; and T.L. was supported by an NIH/NIAMS grant [R01AR055926]. Deposited in PMC for release after 12 months.

References

Andrew, D. J. and Ewald, A. J. (2010). Morphogenesis of epithelial tubes: Insights into tube formation, elongation, and elaboration. *Dev. Biol.* **341**, 34-55.

Aranda, V., Haire, T., Nolan, M. E., Calarco, J. P., Rozenberg, A. Z., Fawcett, J. P., Pawson, T. and Muthuswamy, S. K. (2006). Par6-aPKC uncouples ErbB2 induced

disruption of polarized epithelial organization from proliferation control. *Nat. Cell Biol.* **8**, 1235-1245.
Belteki, G., Haigh, J., Kabacs, N., Haigh, K., Sison, K., Costantini, F., Whitsett, J., Quaggin, S. E. and Nagy, A. (2005). Conditional and inducible transgene expression in mice through the combinatorial use of Cre-mediated recombination and tetracycline induction. *Nucleic Acids Res.* **33**, e51.
Bryant, D. M. and Mostov, K. E. (2008). From cells to organs: building polarized tissue. *Nat. Rev. Mol. Cell Biol.* **9**, 887-901.
Edelstein, A., Amodaj, N., Hoover, K., Vale, R. and Stuurman, N. (2010). Computer control of microscopes using microManager. *Curr. Protoc. Mol. Biol.* **92**, 14.20.1-14.20.17.
Ewald, A. J. (2013). Practical considerations for long-term time-lapse imaging of epithelial morphogenesis in three-dimensional organotypic cultures. *Cold Spring Harb. Protoc.* **2013**, 100-117.
Ewald, A. J., Brenot, A., Duong, M., Chan, B. S. and Werb, Z. (2008). Collective epithelial migration and cell rearrangements drive mammary branching morphogenesis. *Dev. Cell* **14**, 570-581.
Ewald, A. J., Huebner, R. J., Palsdottir, H., Lee, J. K., Perez, M. J., Jorgens, D. M., Tauscher, A. N., Cheung, K. J., Werb, Z. and Auer, M. (2012). Mammary collective cell migration involves transient loss of epithelial features and individual cell migration within the epithelium. *J. Cell Sci.* **125**, 2638-2654.
Ewing, J. (1933). *Lectures on Tumor Pathology*, 2nd edn. New York, NY: Cornell University Medical School.
Fata, J. E., Mori, H., Ewald, A. J., Zhang, H., Yao, E., Werb, Z. and Bissell, M. J. (2007). The MAPK(ERK-1,2) pathway integrates distinct and antagonistic signals from TGFalpha and FGF7 in morphogenesis of mouse mammary epithelium. *Dev. Biol.* **306**, 193-207.
Fuchs, E. (2007). Scratching the surface of skin development. *Nature* **445**, 834-842.
Hadjantonakis, A. K. and Papaioannou, V. E. (2004). Dynamic in vivo imaging and cell tracking using a histone fluorescent protein fusion in mice. *BMC Biotechnol.* **4**, 33.
Hanahan, D. and Weinberg, R. A. (2011). Hallmarks of cancer: the next generation. *Cell* **144**, 646-674.
Hennighausen, L. and Robinson, G. W. (2005). Information networks in the mammary gland. *Nat. Rev. Mol. Cell Biol.* **6**, 715-725.
Hinck, L. and Silberstein, G. B. (2005). Key stages in mammary gland development: the mammary end bud as a motile organ. *Breast Cancer Res.* **7**, 245-251.
Hogg, N. A., Harrison, C. J. and Tickle, C. (1983). Lumen formation in the developing mouse mammary gland. *J. Embryol. Exp. Morphol.* **73**, 39-57.
Hsu, J. C. and Yamada, K. M. (2010). Salivary gland branching morphogenesis – recent progress and future opportunities. *Int. J. Oral Sci.* **2**, 117-126.
Huang, L. and Muthuswamy, S. K. (2010). Polarity protein alterations in carcinoma: a focus on emerging roles for polarity regulators. *Curr. Opin. Genet. Dev.* **20**, 41-50.
Kieserman, E. K. and Wallingford, J. B. (2009). In vivo imaging reveals a role for Cdc42 in spindle positioning and planar orientation of cell divisions during vertebrate neural tube closure. *J. Cell Sci.* **122**, 2481-2490.
Lechler, T. and Fuchs, E. (2005). Asymmetric cell divisions promote stratification and differentiation of mammalian skin. *Nature* **437**, 275-280.
Leung, C. T. and Brugge, J. S. (2012). Outgrowth of single oncogene-expressing cells from suppressive epithelial environments. *Nature* **482**, 410-413.
Mailleux, A. A., Overholtzer, M., Schmelzle, T., Bouillet, P., Strasser, A. and Brugge, J. S. (2007). BIM regulates apoptosis during mammary ductal morphogenesis, and its absence reveals alternative cell death mechanisms. *Dev. Cell* **12**, 221-234.
McCaffrey, L. M. and Macara, I. G. (2009). The Par3/aPKC interaction is essential for end bud remodeling and progenitor differentiation during mammary gland morphogenesis. *Genes Dev.* **23**, 1450-1460.
McNally, S. and Martin, F. (2011). Molecular regulators of pubertal mammary gland development. *Ann. Med.* **43**, 212-234.
Muthuswamy, S. K., Li, D., Lelievre, S., Bissell, M. J. and Brugge, J. S. (2001). ErbB2, but not ErbB1, reinitiates proliferation and induces luminal repopulation in epithelial acini. *Nat. Cell Biol.* **3**, 785-792.
Muzumdar, M. D., Tasic, B., Miyamichi, K., Li, L. and Luo, L. (2007). A global double-fluorescent Cre reporter mouse. *Genesis* **45**, 593-605.
Nanba, D., Nakanishi, Y. and Hieda, Y. (2001). Changes in adhesive properties of epithelial cells during early morphogenesis of the mammary gland. *Dev. Growth Differ.* **43**, 535-544.
Nelson, W. J. (2003). Adaptation of core mechanisms to generate cell polarity. *Nature* **422**, 766-774.
Nelson, W. J. (2009). Remodeling epithelial cell organization: transitions between front-rear and apical-basal polarity. *Cold Spring Harb. Perspect. Biol.* **1**, a000513.
Nguyen-Ngoc, K. V., Shamir, E. R., Huebner, R. J., Beck, J. N., Cheung, K. J. and Ewald, A. J. (2014). 3D culture assays of murine mammary branching morphogenesis and epithelial invasion. *Methods Mol. Biol.* (in press).
Regan, J. L., Sourisseau, T., Soady, K., Kendrick, H., McCarthy, A., Tang, C., Brennan, K., Linardopoulos, S., White, D. E. and Smalley, M. J. (2013). Aurora A kinase regulates mammary epithelial cell fate by determining mitotic spindle orientation in a Notch-dependent manner. *Cell Rep.* **4**, 110-123.
Rhyu, M. S., Jan, L. Y. and Jan, Y. N. (1994). Asymmetric distribution of numb protein during division of the sensory organ precursor cell confers distinct fates to daughter cells. *Cell* **76**, 477-491.
Schneeberger, E. E. and Lynch, R. D. (2004). The tight junction: a multifunctional complex. *Am. J. Physiol.* **286**, C1213-C1228.
Srinivasan, L., Sasaki, Y., Calado, D. P., Zhang, B., Paik, J. H., DePinho, R. A., Kutok, J. L., Kearney, J. F., Otipoby, K. L. and Rajewsky, K. (2009). PI3 kinase signals BCR-dependent mature B cell survival. *Cell* **139**, 573-586.
Sternlicht, M. D. (2006). Key stages in mammary gland development: the cues that regulate ductal branching morphogenesis. *Breast Cancer Res.* **8**, 201.
Sternlicht, M. D., Kouros-Mehr, H., Lu, P. and Werb, Z. (2006). Hormonal and local control of mammary branching morphogenesis. *Differentiation* **74**, 365-381.
Taddei, I., Deugnier, M. A., Faraldo, M. M., Petit, V., Bouvard, D., Medina, D., Fässler, R., Thiery, J. P. and Glukhova, M. A. (2008). Beta1 integrin deletion from the basal compartment of the mammary epithelium affects stem cells. *Nat. Cell Biol.* **10**, 716-722.
Tang, N., Marshall, W. F., McMahon, M., Metzger, R. J. and Martin, G. R. (2011). Control of mitotic spindle angle by the RAS-regulated ERK1/2 pathway determines lung tube shape. *Science* **333**, 342-345.
Thiery, J. P. (2002). Epithelial-mesenchymal transitions in tumour progression. *Nat. Rev. Cancer* **2**, 442-454.
Thiery, J. P., Acloque, H., Huang, R. Y. and Nieto, M. A. (2009). Epithelial-mesenchymal transitions in development and disease. *Cell* **139**, 871-890.
Underwood, J. M., Imbalzano, K. M., Weaver, V. M., Fischer, A. H., Imbalzano, A. N. and Nickerson, J. A. (2006). The ultrastructure of MCF-10A acini. *J. Cell. Physiol.* **208**, 141-148.
Vaezi, A., Bauer, C., Vasioukhin, V. and Fuchs, E. (2002). Actin cable dynamics and Rho/Rock orchestrate a polarized cytoskeletal architecture in the early steps of assembling a stratified epithelium. *Dev. Cell* **3**, 367-381.
Vaillant, F., Asselin-Labat, M. L., Shackleton, M., Lindeman, G. J. and Visvader, J. E. (2007). The emerging picture of the mouse mammary stem cell. *Stem Cell Rev.* **3**, 114-123.
Visvader, J. E. and Smith, G. H. (2011). Murine mammary epithelial stem cells: discovery, function, and current status. *Cold Spring Harb. Perspect. Biol.* **3**, a004879.
Williams, J. M. and Daniel, C. W. (1983). Mammary ductal elongation: differentiation of myoepithelium and basal lamina during branching morphogenesis. *Dev. Biol.* **97**, 274-290.
Xie, W., Chow, L. T., Paterson, A. J., Chin, E. and Kudlow, J. E. (1999). Conditional expression of the ErbB2 oncogene elicits reversible hyperplasia in stratified epithelia and up-regulation of TGFalpha expression in transgenic mice. *Oncogene* **18**, 3593-3607.
Yagi, S., Matsuda, M. and Kiyokawa, E. (2012). Suppression of Rac1 activity at the apical membrane of MDCK cells is essential for cyst structure maintenance. *EMBO Rep.* **13**, 237-243.
Yang, J. and Weinberg, R. A. (2008). Epithelial-mesenchymal transition: at the crossroads of development and tumor metastasis. *Dev. Cell* **14**, 818-829.
Yeaman, C., Grindstaff, K. K. and Nelson, W. J. (1999). New perspectives on mechanisms involved in generating epithelial cell polarity. *Physiol. Rev.* **79**, 73-98.
Zegers, M. M., O'Brien, L. E., Yu, W., Datta, A. and Mostov, K. E. (2003). Epithelial polarity and tubulogenesis in vitro. *Trends Cell Biol.* **13**, 169-176.
Zhan, L., Rosenberg, A., Bergami, K. C., Yu, M., Xuan, Z., Jaffe, A. B., Allred, C. and Muthuswamy, S. K. (2008). Deregulation of scribble promotes mammary tumorigenesis and reveals a role for cell polarity in carcinoma. *Cell* **135**, 865-878.